BioSystems 178 (2019) 25–31

Contents lists available at ScienceDirect

BioSystems

journal homepage: www.elsevier.com/locate/biosystems

Multiplicative noise is beneficial for the transmission of sensory signals in simple neuron models

Jonathan Bauermann[a,b], Benjamin Lindner[a,*]

[a] Bernstein Center for Computational Neuroscience Berlin, Philippstr. 13, Haus 2, 10115 Berlin, Germany
[b] Department of Physics, Humboldt Universität zu Berlin, Newtonstrasse 15, 12489 Berlin, Germany

ARTICLE INFO

Keywords:
Stochastic resonance
Multiplicative noise
Stochastic neuron models
Neural information transmission

ABSTRACT

We study simple integrate-and-fire type models with multiplicative noise and consider the transmission of a weak and slow signal, i.e. a signal that evokes a small modulation of the instantaneous firing rate on time scales that are much larger than the membrane time scale and the mean interspike interval. The specific question of interest is whether and how the state-dependence of the noise can be optimized with respect to information transmission. First, in a simple model in which the noise intensity varies linearly with the state variable, we show analytically that multiplicative fluctuations may benefit the signal transfer and we elucidate the mechanism for this improvement. In a conductance-based integrate-and-fire model with synaptically filtered shot-noise input, we show by means of extended numerical simulations that also in a biophysically more relevant situation, multiplicative noise can enhance the signal-to-noise ratio. Our results shed light on a so far unexplored aspect of stochastic signal transmission in neural systems.

1. Introduction

In nonlinear systems the presence of fluctuations can be advantageous to the transmission of a signal. This effect is best known in the form of stochastic resonance (sometimes also referred to as stochastic facilitation) and has been thoroughly studied since the early 1990s (for reviews, see Anishchenko et al., 1999; Gammaitoni et al., 1998, 2009; McDonnell and Ward, 2011). The effect has gained some popularity especially in neuroscience because neurons respond in an inherently nonlinear all-or-none fashion to external stimuli, they are subject to several sources of noise, and they are thought of as information-transmission devices – hence, they meet all the requirements for stochastic resonance.

How can random fluctuations, i.e. noise help to transmit a weak signal? The basic idea is simple: If the signal is too weak to elicit any response in the strongly nonlinear system, e.g. it is too weak to evoke an action potential in an excitable neuron, a little bit of noise can help to get at least some response that will in general be correlated with the driving signal. Too much noise may reduce the correlation or it may induce too much trial-to-trial variability that makes is hard to see the signal in the output.

In the overwhelming majority of studies, the fluctuations act irrespective of the state that the system currently occupies – the noise is *additive*. There are many systems, however, including nerve cells for which fluctuations enter the dynamics with a factor that depends on the state of the driven system. For neurons, synaptic input from other cells, for instance, arrives as a change in conductance that enters the voltage dynamics of the postsynaptic cell via the electromotive force that depends in a linear fashion on the voltage of the neuron. If neurons are subject to different kinds of synapses (either excitatory or inhibitory or in general simply differing in their reversal potentials), a more general voltage dependence of the noise is possible.

From a stochastic-dynamics point of view, it is interesting whether one could add the noise specifically in places where it is needed to increase the neuron's firing rate or to reduce it in places where such a reduction can enhance the sensitivity with respect to a weak signal. Multiplicative noise can lead to a number of interesting stochastic effects, e.g. noise-induced transitions in which multiplicative noise leads to new maxima in the probability density (Horsthemke and Lefever, 1983) or the blowtorch effect for Brownian motion in periodic potentials in which multiplicative noise can induce a drift motion in a system without macroscopic bias (Büttiker, 1987) to name but two classical examples.

Some studies have already examined stochastic resonance in the presence of multiplicative noise. In a bistable potential, the beneficial effect of additive noise was suppressed for higher noise amplitudes if additionally, independent multiplicative noise (modulating the anharmonic part of the potential) was added to the system (Bulsara et al.,

* Corresponding author at: Bernstein Center for Computational Neuroscience Berlin, Philippstr. 13, Haus 2, 10115 Berlin, Germany.
E-mail address: benjamin.lindner@physik.hu-berlin.de (B. Lindner).

https://doi.org/10.1016/j.biosystems.2019.02.002
Received 24 October 2018; Received in revised form 27 January 2019; Accepted 4 February 2019
Available online 05 February 2019
0303-2647/

1991). This is related to an effective reduction of the potential barrier in the bistable system if this type of multiplicative noise is present (Bulsara et al., 1989). It was also shown that a multiplicative noise with linear dependence of its amplitude on the state variable can lead to stochastic resonance in bistable systems (Gammaitoni et al., 1994) and, if it is a temporally correlated noise, even in linear systems (Fuliński, 1995; Berdichevsky and Gitterman, 1996).

From a neurobiological point of view, it is relevant to learn whether a certain combination of reversal potentials can optimize the signal flow simply because it optimizes the distribution of noise amplitudes in the phase space. Previous experimental work (Marcoux et al., 2016) has already shown voltage dependent fluctuations and discussed the question of its relevance for signal transmission. We will use the concept of multiplicative noise from stochastic-dynamics theory for addressing the same question. Our paper is organized as follows. First, we inspect a simple, analytically tractable linear ramp model (Bulsara et al., 1996), also known as linear integrate-and-fire model (Fusi and Mattia, 1999) that we here study in a version with multiplicative noise and a slow driving signal (slow means that the signal's time scale is large compared to the time scale of the membrane potential and the mean interspike interval); in this model we compute the signal-to-noise ratio by means of first-passage time theory (Section 2). We then turn in Section 3 to the biophysically more realistic model by Stein (1967) in a version in which synaptically filtered Poisson spike trains (including both excitatory and inhibitory synapses) impinge on a conductance-based leaky integrate-and-fire model (Johannesma, 1968). For this model we discuss how to define and quantify the multiplicativity of the noise and show that parameter regimes with stronger multiplicative noise may enable an improved signal transmission. We conclude in Section 4 with a brief summary and discussion of our results.

2. Excitable neuron with multiplicative noise and additive signal

The influence of multiplicative noise on the signal transmission is studied in the simplest integrate-and-fire neuron that shows excitability. Bulsara et al. (1996) and Fusi and Mattia (1999) introduced this model as so-called linear ramp model or linear integrate-and-fire neuron, respectively, and studied mean ISI, its coefficient of variation (CV) and the ISI distribution with a pure white noise driving (Fusi and Mattia, 1999) and some of these statistics under a periodic forcing (Bulsara et al., 1996). Here we endow the model with a simple multiplicative (voltage-dependent) white Gaussian noise and a weak periodic driving and inspect the transmission of the periodic signal.

The dynamics of the neuron's membrane potential v is given by

$$\dot{v} = -\alpha + \varepsilon \sin(2\pi f_s t + \phi) + \sqrt{2D(v)}\,\xi(t), \tag{1}$$

where time is measured in units of the membrane time constant (a typical value is 10 ms). The term $-\alpha$ can be regarded as the negative slope of a simple ramp potential, $U(v) = \alpha v$ (see Fig. 1a) that has a reflecting boundary at $v_R = 0$; furthermore, the dynamics obeys a fire-and-reset mechanism: whenever the voltage crosses v_T, a spike is registered (the sequence of delta spikes is denoted by $x(t) = \Sigma\delta(t - t_i)$) and the voltage is reset to the reflecting barrier at v_R.

The dynamics is equivalent to an overdamped Brownian particle with position variable v subject to a linear potential $U(v)$ with slope α (see Fig. 1a), to a signal in the form of a periodic driving $s(t) = \varepsilon \sin(2\pi f_s t + \phi)$ (amplitude ε, frequency f_s and a initial phase ϕ), and to position-dependent (multiplicative) temporally uncorrelated (white) Gaussian fluctuations with $\langle \xi(t)\xi(t')\rangle = \delta(t - t')$. For the noise intensity we choose a simple linear function (see Fig. 1b)

$$D(v) = \bar{D} + m\left(v - \frac{v_R + v_T}{2}\right). \tag{2}$$

The first parameter, $\bar{D}$, determines the average noise intensity in the interval, while the latter, m, varies the multiplicativity (the strength of the voltage dependence). Three different settings are shown in Fig. 1b. For $m > 0$ ($m < 0$) the noise increases (decreases) linearly with increasing voltage; with $m = 0$, additive noise is obtained. For all multiplicative settings, Eq. (1) is interpreted in the sense of Itô (Gardiner, 1985). We note that the requirement of positive noise intensity leads to the constraint $|m| < 2\bar{D}/(v_T - v_R)$.

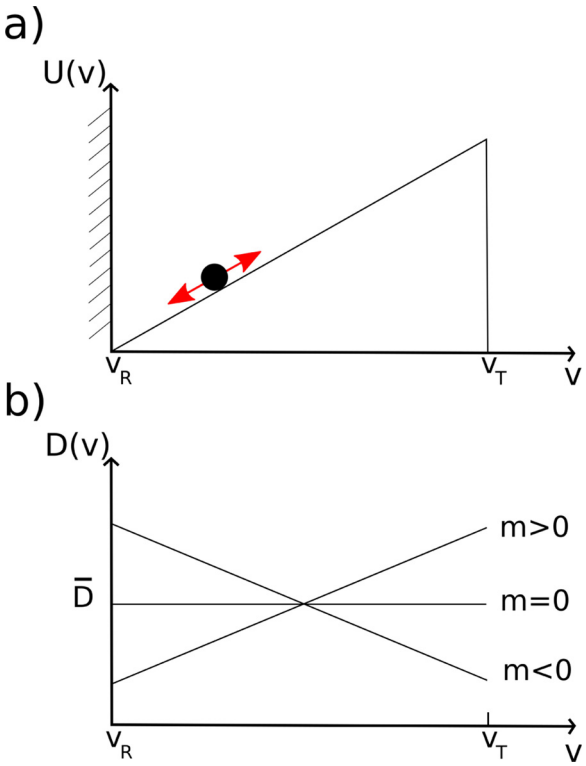

Fig. 1. Sketch of the model: Effective potential with a reflecting barrier on the left and an absorbing barrier on the right (a); the intensity of the driving fluctuations (b) depends in a linear fashion on the state variable v (three possible cases are indicated). Absorption of the particle (black circle) is associated with the generation of a spike (not shown); the temporal sequence of generated spikes is the (signal-encoding) output of the model (see Fig. 2).

In Fig. 2a, an exemplary trajectory of the model is shown. The voltage (green) is driven by a slow and weak signal (red) and noise (not shown); spike times (threshold crossings followed by resets) are indicated by arrows – these spikes encode the signal and how well they do so can be quantified in terms of the power spectrum, Fig. 2b. The latter

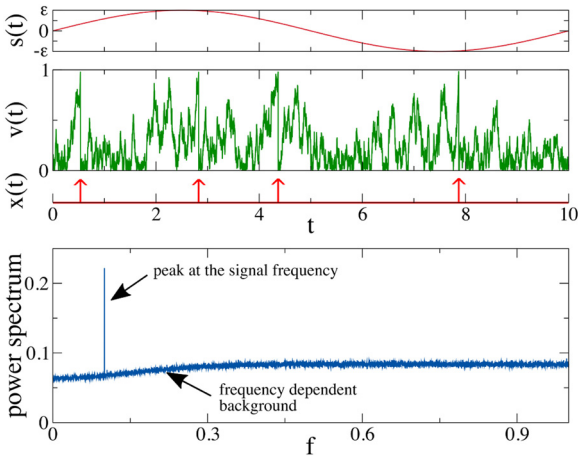

Fig. 2. Signal, voltage, output, power spectrum, $v_R = 0$, $v_T = 1$, $\alpha = 1$, $\varepsilon = 0.1$, $\bar{D} = 0.5$, $m = 0$, $\Delta t = 10^{-4}$, power spectrum: $T_{sim} = 2^{27} \cdot \Delta t$.

is for a finite simulation (or observation) window T_{sim} defined by

$$S(f) = \frac{\langle \tilde{x}\tilde{x}^* \rangle}{T_{\text{sim}}} \tag{3}$$

where $\tilde{x} = \int_0^{T_{\text{sim}}} \mathrm{d}t e^{2\pi i\, ft} x(t)$ is the Fourier transform, the asterisk denotes the complex conjugated, and the angular brackets indicate an ensemble average over the noise $\xi(t)$ and the driving's initial phase (which is drawn from a uniform distribution in $[0, 2\pi)$).

Under a periodic driving, the power spectrum consists of a broad background noise floor and a discrete peak at the driving frequency $f_s = 0.1$. How well the signal is transmitted is quantified by how much the peak sticks out of the noise floor which on a logarithmic scale is quantified by the signal-to-noise ratio (SNR) (McNamara and Wiesenfeld, 1989; Stemmler, 1996; Gammaitoni et al., 1998). The SNR can be defined as

$$\mathrm{SNR}(f_s) = \frac{4}{\varepsilon^2 T_{\text{sim}}} \frac{S_p(f_s)}{S_{\text{bg}}(f_s)} = \frac{4}{\varepsilon^2 T_{\text{sim}}} \frac{S(f_s) - S_{\text{bg}}(f_s)}{S_{\text{bg}}(f_s)}, \tag{4}$$

where T_{sim} is the length of the observation (or simulation) time, $S_{bg}(f_s)$ is the background power at the signal frequency and $S_p(f_s)$ the peak height. With this definition, the SNR quantifies the capability of detecting the weak and slow signal in the output; the chosen prefactor eliminates the simple dependences on the signal strength ε (at least, for a sufficiently weak signal (Voronenko and Lindner, 2017)) and on the observation time T_{sim}.

Fortunately, the model is so simple that an analytical approximation of the SNR is feasible. If we assume that the signal is very slow, we can use linear-response theory and point-process theory to obtain an expression in terms of the moments of the model's interspike interval:

$$\mathrm{SNR} = \lim_{f_s \to 0} \mathrm{SNR}(f_s) = \frac{\left|\frac{\partial r_0}{\partial \alpha}\right|^2}{r_0 C_v^2} = \frac{\left|\frac{\partial \langle I \rangle}{\partial \alpha}\right|^2}{\langle I \rangle \langle \Delta I^2 \rangle}. \tag{5}$$

Here r_0 is the spontaneous firing rate (the inverse of the mean ISI, $r_0 = 1/\langle I \rangle$) and $C_v = \sqrt{\langle \Delta I^2 \rangle}/\langle I \rangle$ is the coefficient of variation of the interspike interval I, both in the absence of the periodic driving ($\varepsilon = 0$). The numerator is related to the linear response function (susceptibility) $\chi(0) = \left|\frac{\partial r_0}{\partial \alpha}\right|$ in the low-frequency limit: this function is given by the slope of the firing-rate vs. input current curve (Stemmler, 1996; Lindner, 2002). The denominator expresses the power spectrum of the unperturbed system's spike train (a so-called renewal point process) by rate and C_v.

Mathematically, the interspike interval corresponds to the first-passage time from reset point to threshold; its moments can be calculated by standard quadrature formulas. In general, the n'th moment $T_n(x) = \langle T^n(x \to v_T) \rangle$ of the first-passage time distribution from any starting point x to the threshold can be computed in an iterative manner (Gardiner, 1985):

$$T_n(x) = n \int_x^{v_T} \frac{\mathrm{d}y}{\psi(y)} \int_{v_R}^{y} \mathrm{d}z \frac{T_{n-1}(z)\psi(z)}{D(z)}, \tag{6}$$

where $\psi(x) = \exp\left(-\int_{v_R}^{x} \mathrm{d}x' \frac{\alpha}{D(x')}\right)$ and $T_0(x) = 1$. Applying these formulas to our simple problem, we can calculate the integrals explicitly yielding for the mean ISI

$$\langle I \rangle = \frac{D_R}{\alpha(\alpha + m)} \left[\left(\frac{D_T}{D_R}\right)^{\frac{\alpha}{m}+1} - 1 \right] - \frac{\Delta v}{\alpha}, \tag{7}$$

where $D_R = D(v_R)$, $D_T = D(v_T)$ and $\Delta v = v_T - v_R$. We note that the limit of an additive noise ($m = 0$) which has been treated in the literature (Fusi and Mattia, 1999) is not completely trivial: one has to take specifically

$$\left(\frac{D_T}{D_R}\right)^{\frac{\alpha}{m}+1} = \left(\frac{\bar{D} + m\Delta v/2}{\bar{D} - m\Delta v/2}\right)^{\frac{\alpha}{m}+1} \xrightarrow{m \to 0} \exp\left[\frac{\alpha \Delta v}{\bar{D}}\right]. \tag{8}$$

If we use this expression in Eq. (7), we obtain for the inverse of the mean ISI, the firing rate,

$$r_0(m=0) = \frac{\alpha^2/\bar{D}}{e^x - x - 1}, \quad x = \frac{\alpha v_T}{\bar{D}}. \tag{9}$$

This agrees with the expression by Fusi and Mattia (1999) if we consider in their formula a vanishing absolute refractory period, $\tau_{arp} = 0$ (such a period was not included in our model).

Returning to the general case of a multiplicative noise ($m \neq 0$), we obtain by the evaluation of the quadratures for the variance:

$$\begin{aligned}\langle \Delta I^2 \rangle = {} & \frac{D_R^2}{\alpha^2(\alpha+m)^2} \left[\left(\frac{D_T}{D_R}\right)^{\frac{\alpha}{m}+1} - 1 \right]^2 \\ & + \frac{2D_R}{\alpha(\alpha+2m)} \left(\frac{D_T}{D_R}\right)^{\frac{\alpha}{m}+1} \left[\frac{3D_R}{\alpha^2 - m^2} - \frac{2\Delta v}{\alpha} \right] - \frac{\Delta v (D_R + D_T)}{\alpha^2(\alpha - m)} \\ & - \frac{6D_R^2}{\alpha(\alpha^2 - m^2)(\alpha + 2m)}.\end{aligned} \tag{10}$$

Also here, we can perform the limit $m \to 0$, using Eq. (8), leading to

$$\langle \Delta I^2 \rangle (m=0) = \frac{\bar{D}^2}{\alpha^4} [e^{2x} + 4e^x(1-x) - 2x - 5] \tag{11}$$

which, together with Eq. (9), results in the expression for the C_v derived by Fusi and Mattia (1999) (assuming again their absolute refractory period to be zero).

Finally, the derivative of $\langle I \rangle$ (given in Eq. (7)) with respect to α is given by

$$\begin{aligned}\frac{\partial \langle \mathrm{ISI} \rangle}{\partial \alpha} = {} & \frac{D_T \left(\frac{D_T}{D_R}\right)^{\frac{\alpha}{m}}}{\alpha^2(\alpha+m)} \left[\ln\left(\frac{D_T}{D_R}\right) \frac{\alpha}{m} - \frac{m + 2\alpha}{\alpha + m} \right] + \frac{D_T(m+2\alpha)}{\alpha^2(\alpha+m)^2} \\ & + \frac{\Delta v}{(\alpha+m)^2}.\end{aligned} \tag{12}$$

Inserting all of these expressions into Eq. (5), we obtain an explicit but not very illuminating formula (not shown, limit cases of this formula will be however discussed below). In Fig. 3 we compare the analytical approximation for $\alpha = 1$, $v_R = 0$ and $v_T = 1$ to numerical simulations of the SNR (symbols) with a low but non-vanishing frequency ($f_s = 0.1$) and small amplitude ($\varepsilon = 0.05$) of the periodic driving. In the simulations, we used Eq. (4) from $N = 500$ runs with randomly chosen signal phase, ϕ, (cf. the discussion of these numerical issues in McNamara and Wiesenfeld, 1989). The comparison reveals the robustness of our adiabatic linear response result – it is neither very sensitive to the value of the driving frequency (as long as the driving is sufficiently slow) nor to the amplitude (as long as it is sufficiently small). For recent studies of the nonlinear response of IF models, see Voronenko and Lindner (2017)

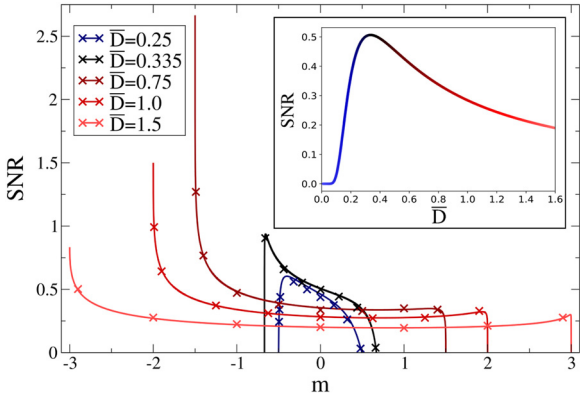

Fig. 3. SNR versus slope of noise function m for different $\bar{D}$. Theory (line), Eq. (5), compared to the SNR extracted from simulation results via Eq. (4) (symbols). Inset: SNR versus $\bar{D}$, additive case ($m = 0$), parameters: $v_R = 0$, $v_T = 1$, $\alpha = 1$, $\varepsilon = 0.05$, $N = 500$, $\Delta t = 10^{-4}$–10^{-5}, $T_{sim} = 2^{27} \cdot \Delta t$, $f_{sig} = 0.1$.

and Voronenko and Lindner (2018).

We made sure that the excitable neuron shows classical stochastic resonance for an additive noise ($m = 0$). In this case, this function reads

$$\mathrm{SNR}_{\mathrm{add}} = \frac{[(x-2)e^x + x + 2]/\bar{D}}{(e^x - x - 1)(e^{2x} + 4(1-x)e^x - 2x + 5)}, \tag{13}$$

where we used again $x = \alpha\Delta v/\bar{D}$. If we fix the voltage and time scales such that $\alpha = 1$ and $\Delta v = 1$, this SNR becomes a function of $\bar{D}$ alone that attains a single maximum of about 0.5064 at $D \approx 0.335$ (cf. inset of Fig. 3) which is the stochastic resonance.

Remarkably, higher SNR values than in the additive case can be obtained using multiplicative noise settings ($m \neq 0$, see Fig. 3). Choosing five different noise levels (including the optimal noise intensity in the additive case), we vary the value of m. The analytical approximation of the SNR versus the slope m of the noise function is shown by solid lines. Their colors reflect the value of $\bar{D}$, set equal to the noise intensity in the additive case shown in the inset (the optimal value corresponds to the black curve). Note that all results are constrained by $|m| < 2\bar{D}/(v_T - v_R)$ (otherwise the noise intensity would attain unphysical negative values).

Clearly, the signal transmission is enhanced for negative slope values of m. For $m < 0$, the noise is stronger close to the reflecting boundary on the left hand side and, speaking in terms of the Brownian-particle analogy, it becomes simpler for the particle to escape from the vicinity of the potential minimum than in the case of additive noise. However, once the voltage has reached higher values (the particle comes close to the absorbing threshold), noise is weaker and the weak signal is more dominant in determining when the threshold crossing (and the associated spike) occurs.

From our analytical solution, three different behaviours can be found in the limit $m \to -2\bar{D}/\Delta v$ (the left side of the SNR curve). The SNR falls either off to 0 for sufficiently weak mean noise with $\bar{D} < \alpha\Delta v/2$; it converges against a finite value for sufficiently strong noise, $\bar{D} > \alpha\Delta v/2$, or, in the rather special setting of $\bar{D} = \alpha\Delta v/2$, it diverges. We note that in all cases, for $m \to -2\bar{D}/\Delta v$, the noise intensity at the threshold *vanishes*. For $\bar{D} > \alpha\Delta v/2$, we find a simple expression at the minimal value of $m = m_c = -2\bar{D}/\Delta v$ that reads

$$\mathrm{SNR}_c = \frac{1 + m_c/\alpha}{2\bar{D}(1 + m_c/\alpha)} = \frac{\alpha\Delta v - 4\bar{D}}{2\bar{D}[\alpha\Delta v - 2\bar{D}]}. \tag{14}$$

From this expression it becomes apparent that in the setting with multiplicative noise we may achieve an arbitrary high SNR by first turning the slope of the noise function into a function of $\bar{D}$ and then letting $\bar{D}$ go to the critical value $\alpha\Delta v/2$. In particular, as also observed in our numerical simulations with nonvanishing driving frequency and amplitude, we can reach significantly higher SNR values than for the additive-noise case, Eq. (13). Of course, we should be aware that the validity of this result is limited to the linear response and the slow-signal approximation, i.e. increasing the SNR much more than shown in our numerical simulations may require to lower the signal amplitude (and possibly frequency).

In general, this section has demonstrated that voltage-dependent noise can lead to higher SNR values than are possible in the case of purely additive noise. This effect will be studied in the next section in a biophysically more realistic neuron model.

3. Stein's model with synaptically filtered shot noise

We now turn to a model, in which multiplicative noise emerges in the form of time-dependent changes of the synaptic conductances in the current balance equation. This is an extended version of the model by Stein (1967), one of the earliest stochastic neuron models that has been intensely studied in terms of the diffusion approximation (Hanson and Tuckwell, 1983; Lánský and Lánská, 1987). We use the model with synaptically filtered Poisson processes for two types of synapses, excitatory and inhibitory ones (Richardson and Gerstner, 2005), and

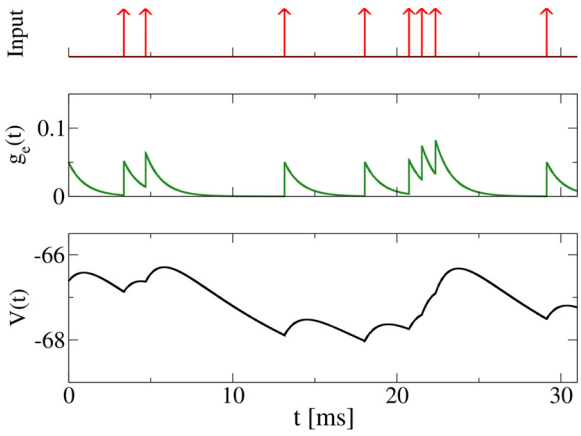

Fig. 4. Stein's model with reversal potentials and low-pass filtered conductance pulses. Input spikes (red, top) that cause jump-like increases in the conductance (green, middle) and smooth changes in the voltage (black, bottom). All evoked activity is subthreshold for this example (no output spikes); a pronounced multiplicative effect is evident by comparing the effect of the first spike to that around $t \approx 13$ ms. Parameters: $C = 0.1$ nF, $E_l = -70$ mV, $E_e = -50$ mV, $g_L = 9.0$ nS, $c_e = 5$ nS, $c_i = 0.0$ nS, $\tau_e = 1.0$ ms and $r_e = 500$ Hz, $\Delta t = 10^{-3}$ ms.

consider as before a weak and slow sinusoidal current stimulus $s(t)$. The equations read

$$C\dot{v} = -g_L(v - E_L) - g_e(v - E_e) - g_i(v - E_i) + s(t), \tag{15}$$

$$\tau_{e,i}\dot{g}_{e,i} = -g_{e,i} + c_{e,i}\tau_{e,i}\sum_j \delta(t - t_{j_e j_i}), \tag{16}$$

where C is the capacitance and g_L the leak conductance of the membrane. The parameters E_L, E_e and E_i are the leak, the excitatory and the inhibitory reversal potentials. The second line represents auxiliary filter dynamics that implement a low-pass filter of the incoming excitatory and inhibitory Poissonian spike trains (rates for the latter are denoted by r_e or r_i, respectively). Each incoming pulse causes a jump-like increase c_e or c_i of the conductance which subsequently decays exponentially with the time scale τ_e and τ_i, respectively. An example of a stochastic simulation of the model with exclusively excitatory input is shown in Fig. 4 and reveals the multiplicative character of the noise.

The firing criterion is as in the last subsection a reset-and-fire rule. Every time the voltage reaches a certain threshold v_T, we register a spike and reset the voltage to v_R. For a noise-driven spiking of the model, it has to be $E_e > v_T$ for the excitatory reversal potential. Because all terms in Eq. (15) depend only linearly on the voltage, we can shift and rescale the voltage and reversal potentials such that we may set $v_R = 0$ and $v_T = 1$ without loss of generality.

For high input rates ($\tau_{e,i}r_{e,i} \gg 1$) and low amplitudes, the Poissonian shot noise in the conductance equations can be approximated by a white Gaussian noise with the same mean value and noise intensity (see e.g. Lánský, 1984; Richardson and Gerstner, 2005 as well as the text books (Holden, 1976; Ricciardi, 1977) and references therein). After this approximation, the dynamics read (Richardson and Gerstner, 2005)

$$\begin{aligned} C\dot{v} &= -g_0(v - E_0) - g_{e;F}(v - E_e) - g_{i;F}(v - E_i) + s, \\ \tau_{e,i}\dot{g}_{ef,i;F} &= -g_{e,i;F} + \sqrt{c_{e,i}^2\tau_{e,i}^2 r_{e,i}}\,\xi_{e,i}. \end{aligned} \tag{17}$$

Here, $g_0 = g_L + c_e\tau_e r_e + c_i\tau_i r_i$ is the mean conductance and $E_0 = (g_L E_L + c_e\tau_e r_e E_e + c_i\tau_i r_i E_i)/g_L$ the resting potential which incorporate already the average effect of the synaptic conductances. Fluctuations are described by the two Ornstein–Uhlenbeck processes which are driven by white Gaussian noise sources with vanishing mean value $\langle\xi_{e,i}(t)\rangle = 0$ and a correlation function $\langle\xi_{e,i}(t)\xi_{e,i}(t')\rangle = \delta(t - t')$. If the correlation times of the two processes $\tau_{e,i}$ are negligible, the problem can be further simplified by approximating the conductance

fluctuations by white noise, $g_{e,i;F} \approx \sqrt{c_{e,i}^2 \tau_{e,i}^2 r_{e,i}} \xi_{e,i}$. After rescaling the whole process in the membrane time scale τ_m, the final diffusion approximation of the dynamics reads

$$\dot{v} = -v + \mu + s(t) + \sqrt{\gamma(\alpha(v-\beta)^2 + 1)}\xi(t), \tag{18}$$

and $s(t) = \varepsilon \sin(2\pi f_{sig} t + \phi)$. [It should be mentioned, that in this approximation voltage values below the inhibitory reversal potential are possible due to the nature of the Gaussian noise (Lánský and Lánská, 1987). This is not possible in Stein's model, Eq. (15).] The new parameters are related to the original model, Eq. (16) via:

$$\begin{aligned}
\tau_m &= \frac{C}{g_L + c_e \tau_e r_e + c_i \tau_i r_i}, \\
\mu &= \frac{g_L E_L + c_e \tau_e r_e E_e + c_i \tau_i r_i E_i}{g_l + c_e \tau_e r_e + c_i \tau_i r_i}, \\
\alpha &= \frac{\left(\frac{c_e \tau_e \sqrt{r_e}}{c_i \tau_i \sqrt{r_i}} + \frac{c_i \tau_i \sqrt{r_i}}{c_e \tau_e \sqrt{r_e}}\right)^2}{(E_e - E_i)^2}, \\
\beta &= \frac{c_e^2 \tau_e^2 r_e E_e + c_i^2 \tau_i^2 r_i E_i}{c_e^2 \tau_e^2 r_e + c_i^2 \tau_i^2 r_i}, \\
\gamma &= \frac{\tau_m}{C^2} \frac{c_e^2 \tau_e^2 r_e c_i^2 \tau_i^2 r_i (E_e - E_i)^2}{c_e^2 \tau_e^2 r_e + c_i^2 \tau_i^2 r_i}.
\end{aligned} \tag{19}$$

The parameter μ captures the resting potential of this neuron, γ is the overall noise intensity. The remaining two parameters describe the multiplicative contribution: a parabola with prefactor α and a minimum at β. Conveniently, $\alpha \geq 0$ parametrizes the strength of the 'multiplicativity'; in particular, for $\alpha = 0$ we recover the case of an LIF neuron with additive white Gaussian noise. We note that in the multiplicative case ($\alpha > 0$), the stochastic differential Eq. (18) has to be interpreted in the Stratonovich sense because of the Wong-Zakai theorem that states that this is the correct interpretation if the driving white-noise process can be thought of as the limit of an correlated noise the correlation time of which vanishes (Wong and Zakai, 1965). We emphasize that the above derivation is far from being novel or original (see the above references on the diffusion approximation) but was included here only for completeness.

As demonstrated in Richardson and Gerstner (2005), taking into account the multiplicative nature of the noise but neglecting the shot-noise character is not consistent in general. We will nevertheless use the approximation to study when the multiplicativity of noise alone can have a beneficial effect on the transmission of the periodic signal. As mentioned before, in the special case $\alpha = 0$, the approximate dynamics Eq. (18) corresponds to a leaky integrate-and-fire neuron with additive noise, a model for which it is known that it exhibits the stochastic resonance effect in the slow-signal limit (Stemmler, 1996) but also for arbitrary high frequencies (Lindner and Schimansky-Geier, 2001). Hence, our question can be rephrased to whether the SNR can be increased by having $\alpha > 0$.

In Fig. 5, we present results for the SNR obtained via Eq. (4) from numerical simulations of Eq. (18). The SNR is displayed as a function of the noise intensity γ for various combinations of the multiplicativity parameters α and β. For a comparatively weak multiplicativity, $\alpha = 0.25$, the curves for different β practically collapse on one line that is very close to the theoretical curve for the additive-noise case (here we employed the exact non-adiabatic result from Lindner and Schimansky-Geier (2001)); we used a small value of α to illustrate that a weakly multiplicative noise does not lead to significant deviations from the additive-noise case (in this sense, the latter is robust).

Remarkably, for a large value of α, i.e. a pronounced multiplicativity, the SNR deviates strongly from the additive case. If $\beta \leq \mu$, the maximal SNR is significantly *larger* than in the additive case, implying that the increased intensity of the noise between resting potential and threshold is helpful for the signal transmission. If, on the contrary, the minimal noise intensity is shifted to the region between resting potential μ and threshold, v_T, ($\beta = 0.95$), the multiplicative character of the noise is detrimental to the signal transmission and the

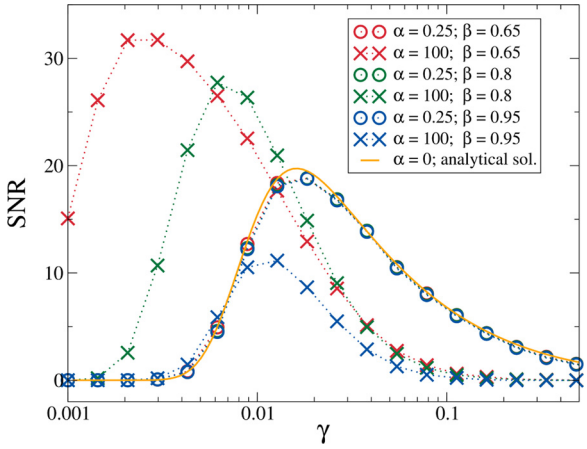

Fig. 5. The signal-to-noise ratio for the approximate model (diffusion approximation), Eq. (18), displays stochastic resonance, i.e. a maximum as a function of the noise intensity γ for various combinations of α and β as indicated. Remarkably, if $\beta < \mu$, the maximum is larger for multiplicative noise ($\alpha = 100$) than for the additive case (with a small value $\alpha = 0.25$); the latter case is also compared to the exact solution from Lindner and Schimansky-Geier (2001). Parameters: $\mu = 0.8$, $v_R = 0$, $v_T = 1$, $f_{sig} = 0.1$, $\varepsilon = 0.02$, $\Delta t = 5 \cdot 10^{-5}$, $t_{sim} = 2^{27} \cdot \Delta t$, $N = 1000$.

SNR suffers an overall reduction.

In the following, we argue that the improved signal transmission due to multiplicative noise can also be found in Stein's model with reversal potentials and low-pass filtered shot-noise conductances. One complication is that the original model does not contain a 'multiplicativity' parameter like the parameter α in the approximate dynamics and that it is not evident how to quantify its 'multiplicativity' in a strict sense if the noise is non-Gaussian and, more importantly in this context, correlated in time. This also relates to the interesting and data-relevant problem of how to identify a multiplicative noise in a time series, say a number of discrete voltage measurements $v_i = v(t_i)$ (the conductance dynamics is typically not accessible). If the input fluctuations are a temporally correlated ('colored') noise, it turns out that standard approaches like the first two moments of the trajectory's increment statistics do not converge but lead to a vanishing noise intensity (Lehle and Peinke, 2018). More specifically, if we consider the second Kramers-Moyal coefficient (Risken, 1984):

$$D_2(\tilde{v}, \Delta t) = \frac{1}{2\Delta t} \langle ((v(t+\Delta t) - v(t)) - \langle v(t+\Delta t) - v(t) \rangle_{v(t)=\tilde{v}})^2 \rangle_{v(t)=\tilde{v}}, \tag{20}$$

i.e. the second moment of the voltage increment $v(t+\Delta t) - v(t)$ conditioned on the prescribed initial value of the voltage, $v(t) = \tilde{v}$, the result tends to zero for $\Delta t \to 0$

$$\lim_{\Delta t \to 0} D_2(\tilde{v}, \Delta t) = 0. \tag{21}$$

So, in this strict limit, there is no voltage-dependent amplitude of the noise and hence no 'multiplicativity' of the fluctuations.

It is clear, however, that if the multiplicative-white-noise approximation is meaningful, it should be possible to recover the multiplicative character of the noise also in the original system. For comparatively fast synapses ($\tau_e = \tau_i = 1$ ms), we have used the relations Eq. (19) to find parameters of the original dynamics such that the membrane time constant $\tau_m = 25$ ms, the mean input $\mu = 0.8$, the minimum's position of the noise parabola, $\beta = 0.35$, are all fixed to the specified values but we are able to prescribe $\alpha = 0.25$ or $\alpha = 7$ and to vary the noise intensity γ within a certain range as well (parameters for $\alpha = 7.0$ and $\alpha = 0.25$ can be found in Tables 1 and 2, respectively). The main difference between the more additive case ($\alpha = 0.25$) and the more multiplicative case ($\alpha = 7$) is the choice of the reversal potentials

Table 1
Parameters for the Stein model yielding $\alpha = 7$, $\beta = 0.35$, $\mu = 0.8$, $\tau_m = 25$ ms. Remaining parameters: $C = 0.4$ nF, $e_L = 0.8$, $e_e = 1.39$, $e_i = 0.21$, $\tau_{e,i} = 1.0$ ms, $r_e = 1500$ Hz, $r_i = 199$ Hz. The asterist indicates the parameter values for the corresponding cross in Fig.7.

γ	g_L [nS]	c_e [nS]	c_i [nS]
0.0010	10.39	1.87	14.10
0.0014	9.27	2.24	16.91
0.0021	7.93	2.69	20.28
0.0030	6.32	3.23	24.32
0.0043	4.39	3.87	29.17
0.0062*	2.08	4.64	34.99

Table 2
Parameters for the Stein model yielding $\alpha = 0.25$, $\beta = 0.35$, $\mu = 0.8$, $\tau_m = 25$ ms. Remaining parameters: $C = 0.4$ nF, $e_L = 0.8$, $e_e = 2.85$, $e_i = -1.25$, $\tau_{e,i} = 1.0$ ms, $r_e = 1500$ Hz, $r_i = 960$ Hz. The asterisk indicates the parameter values for the corresponding cross in Fig.7.

γ	g_L [nS]	c_e [nS]	c_i [nS]
0.0010	14.06	0.65	1.01
0.0014	13.68	0.77	1.21
0.0021	13.22	0.93	1.45
0.0030	12.66	1.11	1.74
0.0043	12.00	1.33	2.09
0.0062	11.20	1.60	2.50
0.0089	10.24	1.92	3.00
0.0127	9.09	2.30	3.60
0.0183*	7.71	2.76	4.32
0.0264	6.06	3.31	5.18
0.0379	4.08	3.97	6.21
0.0546	1.70	4.77	7.45

which are both closer to the resting potential in the multiplicative case (see (Wolff and Lindner, 2008, 2010) for a selection of physiologically plausible values of synaptic amplitudes and reversal potentials that yield pronounced multiplicative effects in the voltage dynamics).

We first inspect how the coefficient Eq. (20) depends on the prescribed value of α (cf. Fig. 6). Indeed, for $\alpha = 0.25$ the coefficient is almost flat for most of the relevant voltage range while for $\alpha = 7$ a pronounced parabola emerges the amplitude of which is maximal for an intermediate value of the time step Δt used in the increment analysis. Consistent with the results in Lehle and Peinke (2018), the coefficient attains only small values when the time step becomes significantly smaller than the time scale of the synapses (cf. red lines in Eq. (20) for $\Delta t = 0.5$ ms). We note that we have excluded from the analysis the time bins in which a voltage reset takes place; still, the coefficient's voltage dependence is certainly not a perfect parabola but displays mild boundary effects close to v_R and v_T.

After we have verified the stronger multiplicativity of the noise in the $\alpha = 7$ case, we can now turn to the question whether this value can also lead to a higher SNR. In Fig. 7, results for the original Stein model and for the diffusion approximation are shown for the two values of α. Clearly, the maximal information transmission is achieved for the more multiplicative noise. We also note that the agreement between the SNR curves of the two models is better for $\alpha = 0.25$; the strong inhibitory synaptic amplitudes used for $\alpha = 7$ (cf. Table 1) lead to stronger deviations between the filtered shot-noise case and the multiplicative white-Gaussian-noise approximation.

4. Summary and discussion

We have studied the role of multiplicative noise for the signal transmission of a slow and weak periodic signal in different versions of excitable integrate-and-fire models. In the linear IF model with a ramp potential and a simple linear variation of the noise intensity with voltage, we could derive an explicit expression for the signal-to-noise ratio

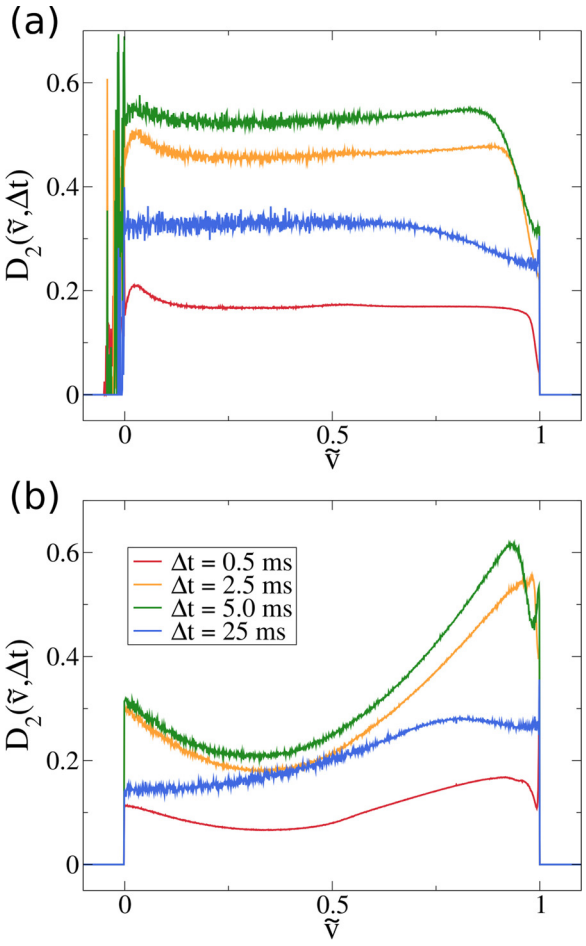

Fig. 6. The Kramers-Moyal-like coefficient, $D_2(v, \Delta t)$, defined in Eq. (20) for different values of the time step as indicated and the parameter sets from Table 1 (a) and Table 2 (b) for the specific noise values $\gamma = 0.0183$ and $\gamma = 0.0062$, respectively.

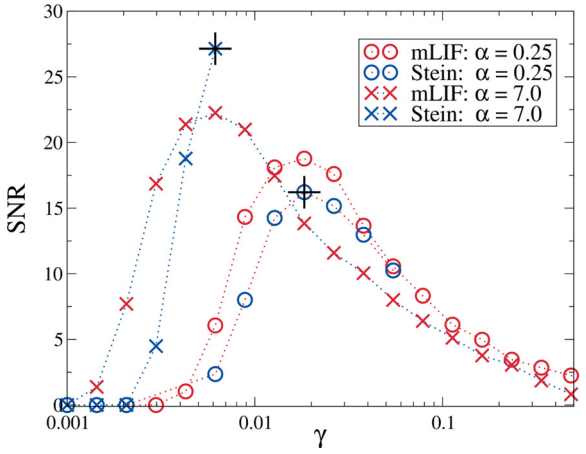

Fig. 7. Numerical results for the SNR of the mLIF model and the original (shot noise) model where it is parameter-wise possible (for higher γ values, the conductivity g_L attains unphysical negative values); + signs indicate the parameter sets used in Fig. (6); parameters: $\beta = 0.35$, $\mu = 0.8$, $v_R = 0$, $v_T = 1$, $f_{sig} = 0.1$, $\varepsilon = 0.02$, $\Delta t = 5 \cdot 10^{-6}$, $t_{sim} = 2^{27}\Delta t$, $n = 750$; parameters for Stein model: see table. Points marked by a cross correspond to the values marked in table 1 and 2 by asterisks.

for a weak and slow cosine signal. The result reveals that an improvement of the SNR is possible if the noise is multiplicative, i.e. its intensity varies with the voltage. Our choice of the neuron model and the noise modulation was here dictated by the wish to construct an analytically tractable example that shows the basic beneficial effect of state-dependent fluctuations on signal transmission.

In the second part we turned to a standard point-neuron model in which a multiplicative noise emerges naturally: if the main source of noise is the random spike train input from other cells, these spikes affect the postsynaptic cell in the form of conductance fluctuations that enter the current balance equation via voltage-dependent prefactors (the electromotive forces). We considered this kind of input entering through populations of excitatory and inhibitory neurons and investigated whether the multiplicative noise can be helpful for the transmission of a weak and slow cosine signal also in this biophysically more relevant case. We found that indeed a more multiplicative setting can lead to higher SNR than a setting in which the fluctuations are closer to an additive noise provided the minimum of the effective noise intensity lays below the resting value of the IF neuron ($\beta \leq \mu$).

In our model we added the signal as a current in Eq. (15). For cortical neurons which communicate mainly via synaptic inputs, it seems more reasonable to consider a signal that modulates one of the rates of the synaptic inputs, r_e or r_i. On the one hand, this leads not only to a modulation of the mean input but also to a modulation of the noise intensity, which has been referred to as a noise-coded signal (Lindner and Schimansky-Geier, 2001) (for more details, see also Lindner, 2002); the transmission of such a signal was shown to also display stochastic resonance with respect to the strength of the additive noise (Lindner and Schimansky-Geier, 2001). On the other hand, a signal that enters through a rate modulation will naturally also come along with a voltage-dependent amplitude, hence we have to deal not only with a multiplicative noise but also with a multiplicative signal.

Returning to our models, the results of the two parts may look contradictory at the first glance. For the simplified noise model, the best signal transmission was achieved for a low value of the input noise close to the threshold – in terms of our linear noise function with slope m, the maximal SNR and even divergences in the SNR could be found for $m < 0$. For the LIF neuron with filtered conductance shot noise, the optimal SNR requires that the multiplicative noise is stronger close to the threshold. We take this as an indication that the effects of multiplicative noise depend a lot on the details: whether the barrier is just a simple slope or a quadratically increasing function, whether detours to strongly negative voltage are possible (LIF neuron) or excluded by a reflecting barrier (linear IF model), whether the noise increases or decreases linearly or varies in a nonlinear and even nonmonotonic fashion can apparently make a big difference for the stochastic dynamics. In addition, these features influence the signal-to-noise ratio both in its denominator (the strength of the spike rate modulation) and in the numerator (the overall variability of the firing). While for the first system (linear IF model and linear noise modulation) it pays off to reduce the noise if the system is close to the threshold, the LIF model with conductance noise seems to profit from an increase of the noise on its way from the resting potential ($v = \mu$) to the threshold ($v = v_T$). A more thorough investigation of the involved mechanisms is desirable but is beyond the scope of our study. It remains certainly an interesting subject for future studies to systematically vary the shapes of drift and diffusion functions and to explore the factors of the shape that determine whether increased or reduced noise close to the threshold of firing is beneficial for the transmission of a weak signal.

An experimental test of our predictions might be feasible via the dynamic-clamp techniques (Sharp et al., 1993; Prinz et al., 2004) by which arbitrary conductances can be mimicked via current injections into a neuron *in vitro*. Testing whether an appropriate change in reversal potentials can lead to an improved signal transmission would be similar to our approach and does not seem to be (conceptually!) very difficult. Whether, for given populations of ion channels with specific reversal potentials, these potentials and the corresponding synaptic amplitudes are already optimized to exploit the multiplicative effect of the noise is another but more complicated question.

References

Anishchenko, V.S., Neiman, A.B., Moss, F., Schimansky-Geier, L., 1999. Phys.-Usp. 42, 7.
Gammaitoni, L., Hänggi, P., Jung, P., Marchesoni, F., 1998. Rev. Mod. Phys. 70, 223.
Gammaitoni, L., Hänggi, P., Jung, P., Marchesoni, F., 2009. Eur. Phys. J. B 69, 1.
McDonnell, M.D., Ward, L.M., 2011. Nat. Rev. Neurosci. 12, 415.
Horsthemke, W., Lefever, R., 1983. Noise-Induced Transitions: Theory and Applications in Physics, Chemistry, and Biology. Springer, Berlin.
Büttiker, M., 1987. Z. Phys. B: Condens. Matter 68, 161.
Marcoux, C., Clarke, S., Nesse, W., Longtin, A., Maler, L., 2016. J. Neurophysiol.
Bulsara, A., Elston, T.C., Doering, C.R., Lowen, S.B., Lindenberg, K., 1996. Phys. Rev. E 53, 3958.
Fusi, S., Mattia, M., 1999. Neural Comput. 11, 633.
Stein, R.B., 1967. Biophys. J. 7, 37.
Johannesma, P.I.M., 1968. In: Caianiello, E.R. (Ed.), Neural Networks. Springer, Berlin.
Gardiner, C.W., 1985. Handbook of Stochastic Methods. Springer-Verlag, Berlin.
Stemmler, M., 1996. Network 7, 687.
Lindner, B., 2002. Coherence and Stochastic Resonance in Nonlinear Dynamical Systems. Logos-Verlag, Berlin.
Voronenko, S., Lindner, B., 2017. New J. Phys. 19, 033038.
McNamara, B., Wiesenfeld, K., 1989. Phys. Rev. A 39, 4854.
Voronenko, S., Lindner, B., 2018. Biol. Cybern. 112, 523.
Hanson, F.B., Tuckwell, H.C., 1983. J. Theor. Neurobiol. 2, 127.
Lánský, P., Lánská, V., 1987. Biol. Cybern. 56, 19.
Lánský, P., 1984. J. Theor. Biol. 107, 631.
Richardson, M.J.E., Gerstner, W., 2005. Neural Comput. 17, 923.
Holden, A.V., 1976. Models of the Stochastic Activity of Neurones. Springer-Verlag, Berlin.
Ricciardi, L.M., 1977. Diffusion Processes and Related Topics on Biology. Springer-Verlag, Berlin.
Lindner, B., Schimansky-Geier, L., 2001. Phys. Rev. Lett. 86, 2934.
Wong, E., Zakai, M., 1965. International Journal of Engineering Science.
Lehle, B., Peinke, J., 2018. Phys. Rev. E 97, 012113.
Risken, H., 1984. The Fokker-Planck Equation. Springer, Berlin.
Wolff, L., Lindner, B., 2008. Phys. Rev. E 77, 041913.
Wolff, L., Lindner, B., 2010. Neural Comput. 22, 94.
Sharp, A.A., O'Neil, M.B., Abbott, L.F., Marder, E., 1993. Trends Neurosci. 16, 389.
Prinz, A.A., Abott, L.F., Marder, E., 2004. Trends Neurosci. 27, 218.
Bulsara, A., Jacobs, E., Zhou, T., Moss, F., Kiss, L., 1991. J. Theor. Biol. 152, 531.
Bulsara, R.D., Boss, A.R., Jacobs, E.W., 1989. Biol. Cybernet. 61, 211.
Gammaitoni, L., Marchesoni, F., Menichella-Saetta, E., Santucci, S., 1994. Phys. Rev. E 49, 4878.
Fuliński, A., 1995. Phys. Rev. E 52, 4523.
Berdichevsky, V., Gitterman, M., 1996. EPL (Europhys. Lett.) 36, 161.